Reversible host cell remodeling underpins deformability changes in malaria parasite sexual blood stages

Megan Dearnley[a,1], Trang Chu[b,1], Yao Zhang[c,1], Oliver Looker[a,1], Changjin Huang[c], Nectarios Klonis[a], Jeff Yeoman[d], Shannon Kenny[a], Mohit Arora[b], James M. Osborne[e], Rajesh Chandramohanadas[b,2], Sulin Zhang[c,2], Matthew W. A. Dixon[a,2], and Leann Tilley[a,2,3]

[a]Department of Biochemistry and Molecular Biology, Bio21 Molecular Science and Biotechnology Institute, University of Melbourne, Melbourne, VIC 3010, Australia; [b]Pillar of Engineering Product Development, Singapore University of Technology and Design, Singapore 487372; [c]Department of Engineering Science and Mechanics, The Pennsylvania State University, University Park, PA 16802; [d]Department of Biochemistry, La Trobe University, Melbourne, VIC 3086, Australia; and [e]School of Mathematics and Statistics, University of Melbourne, Melbourne, VIC 3010, Australia

Edited by Carolina Barillas-Mury, National Institutes of Health, Bethesda, MD, and approved March 4, 2016 (received for review October 22, 2015)

The sexual blood stage of the human malaria parasite *Plasmodium falciparum* undergoes remarkable biophysical changes as it prepares for transmission to mosquitoes. During maturation, midstage gametocytes show low deformability and sequester in the bone marrow and spleen cords, thus avoiding clearance during passage through splenic sinuses. Mature gametocytes exhibit increased deformability and reappear in the peripheral circulation, allowing uptake by mosquitoes. Here we define the reversible changes in erythrocyte membrane organization that underpin this biomechanical transformation. Atomic force microscopy reveals that the length of the spectrin cross-members and the size of the skeletal meshwork increase in developing gametocytes, then decrease in mature-stage gametocytes. These changes are accompanied by relocation of actin from the erythrocyte membrane to the Maurer's clefts. Fluorescence recovery after photobleaching reveals reversible changes in the level of coupling between the membrane skeleton and the plasma membrane. Treatment of midstage gametocytes with cytochalasin D decreases the vertical coupling and increases their filterability. A computationally efficient coarse-grained model of the erythrocyte membrane reveals that restructuring and constraining the spectrin meshwork can fully account for the observed changes in deformability.

gametocyte | deformability | spectrin/actin skeleton | AFM | molecular dynamics simulation

The most virulent of the human malaria parasites, *Plasmodium falciparum* causes ~440,000 deaths annually (1). Pathology is associated with asexual multiplication within red blood cells (RBCs). The trophozoite (growing) and schizont (dividing) stages (~24–48 h after invasion) sequester in deep tissue using adhesive proteins presented on platform-like structures called "knobs" at the infected RBC surface. Cytoadhesion enables the parasite to avoid passage through the splenic sinuses and thus mechanical clearance from the circulation. Unfortunately, complications associated with sequestration of infected RBCs in the brain are responsible for much of the malaria-related mortality and morbidity.

After a period of asexual cycling, a proportion of blood-stage parasites commit to sexual development (gametocytogenesis). The intraerythrocytic gametocyte develops through five distinct stages (I–V) over a period of 10–12 d, eventually adopting the characteristic crescent (falciform) shape that gives *P. falciparum* its name. Elongation is driven by assembly of a sheath of microtubules, attached to an inner membrane complex, underneath the parasite plasma membrane. From stage II to IV, gametocytes disappear from the circulation (2, 3); however, the mechanism of sequestration is not well understood. Upon maturation, the microtubule cytoskeleton is disassembled, and stage V gametocytes re-enter the circulation (2, 3). Ingestion of mature gametocytes by an *Anopheles* mosquito triggers release from the RBCs, followed by sexual recombination in the insect gut, and eventual transmission.

Efforts to control malaria are often thwarted by the presence of gametocytes in asymptomatic individuals. These infected individuals serve as a reservoir during the low transmission season, ready to retransmit disease when mosquito numbers increase. As a consequence, there is intense interest in understanding gametocyte cell biology with the aim of interfering with this developmental stage.

Of particular interest are the molecular and biomechanical changes that accompany the sequestration and release of gametocytes. Developing gametocytes (stages II–IV) have significantly reduced cellular deformability (2, 4, 5). This increased rigidity may enable gametocytes to become mechanically trapped in the bone marrow and splenic cords. In contrast, stage V gametocytes exhibit increased deformability (4–6), which may help them survive in the circulation, where they can be picked up by mosquitoes.

Survival in the circulation requires RBCs to undergo deformation without fragmentation, as they transit through the 1.5- to 2-μm interendothelial slits in the spleen. The remarkable deformability properties of RBCs are thought to derive from their submembranous protein skeleton (7, 8). The skeleton is composed of a regular hexagonal array of spectrin heterodimers that self-associate head-to-head to form tetramers. The tails of

Significance

This study provides, to our knowledge, the first ultrastructural and dynamics analysis of the host red blood cell membrane of *Plasmodium falciparum* gametocytes, revealing reversible expansion of the spectrin–actin skeleton, accompanied by reversible modulation of skeletal coupling to the plasma membrane. We use the measured physical parameters to inform a computationally efficient coarse-grained model. This model shows that restructuring the skeletal meshwork can fully account for the observed deformability changes. We reveal a critical role for actin remodeling in driving this reversible biomechanical host cell subversion. This work provides fundamental insights into the molecular changes that underpin gametocyte survival in the circulation.

Author contributions: R.C., S.L.Z., M.W.A.D., and L.T. designed research; M.D., T.C., Y.Z., O.L., C.J.H., N.K., J.Y., S.K., M.A., and M.W.A.D. performed research; T.C., J.M.O., and R.C. contributed new reagents/analytic tools; M.D., T.C., Y.Z., O.L., C.J.H., N.K., J.Y., J.M.O., R.C., S.L.Z., M.W.A.D., and L.T. analyzed data; and M.D., R.C., S.L.Z., M.W.A.D., and L.T. wrote the paper.

The authors declare no conflict of interest.

This article is a PNAS Direct Submission.

Freely available online through the PNAS open access option.

[1]M.D., T.C., Y.Z., and O.L. contributed equally to this work.

[2]R.C., S.L.Z., M.W.A.D., and L.T. contributed equally to this work.

[3]To whom correspondence should be addressed. Email: ltilley@unimelb.edu.au.

This article contains supporting information online at www.pnas.org/lookup/suppl/doi:10.1073/pnas.1520194113/-/DCSupplemental.

the spectrin heterodimers are linked into junctional complexes containing actin oligomers (each with 14–16 protomers), protein 4.1R, adducin, and accessory proteins (9). Flexible linkages between the triple-helical segments of spectrin heterodimers, as well as tetramer dissociation, and breakable linkages into the junction points, are assumed to accommodate the distortions imposed by shear forces in the circulation.

Vertical interactions connect the skeletal meshwork to the plasma membrane. A subpopulation of band-3 dimers connects to spectrin via ankyrin (9). Band-3 dimers also participate in a second linkage complex that involves glycophorin C. This complex is linked to the membrane skeleton via glycophorin C/protein 4.1 interactions as well as band-3/adducin interactions.

The molecular determinants of the increased rigidity of mature asexual parasite-infected RBCs are beginning to be elucidated. Atomic force microscopy (AFM) has revealed reorganization and expansion of the spectrin network of the host cell membrane (10, 11), while cryo-electron tomography suggests that this reorganization occurs as a result of mining of the actin junctions in order to generate actin filaments that connect parasite-derived organelles known as Maurer's clefts to the knobs (12). A parasite-encoded protein called the Knob-Associated Histidine-Rich Protein (KAHRP) is thought to be a major contributor to RBC rigidification (8, 13). KAHRP binds spectrin and self-assembles into a structure that distorts the RBC membrane with surface protrusions. Recent modeling suggests that composite strengthening and strain hardening of the infected RBC membrane result from modified lateral and vertical interactions within the membrane skeleton and deposition of rigidifying knob structures (8).

In contrast, relatively little is known about host RBC remodeling in gametocytes. There are no knobs on gametocytes, and very limited (if any) surface expression of adhesins (14). In this work, we used AFM to investigate the membrane skeleton structure in gametocyte-infected RBCs and probed the interactions between RBC integral membrane proteins and the membrane skeleton using fluorescence photobleaching. In stage III gametocytes, we observed relocation of actin to Maurer's clefts, accompanied by expansion of the spectrin skeleton and enhanced coupling of the membrane skeleton to the plasma membrane. These changes are reversed in stage V gametocytes. The actin depolymerizing agent cytochalasin D modulates the properties of stage III gametocytes, consistent with reversible actin remodeling. Coarse-grained molecular dynamics (CGMD) modeling reveals that enhanced lateral interactions and constraints on the spectrin motions can fully account for the compromised biomechanical properties of stage III gametocytes.

Results

Disruption of the Gametocyte Microtubule Network Does Not Influence Cellular Deformability. The interstices of a bed of microbeads can provide a physical environment similar to that presented by the fenestrations in the splenic sinuses, permitting passage of deformable RBCs, but trapping RBCs with compromised deformability (15). The ability of asexual *P. falciparum*-infected RBCs to pass through such a filter decreases as the parasite matures to the trophozoite stage (~30 h; Fig. 1). Similarly, stage III gametocytes become trapped in the mesh of the beads. By contrast, stage V gametocytes traverse the filter much more readily, indicating an increase in cellular deformability.

To assess the contribution of the parasite cytoskeleton to the compromised filterability, we treated stage III gametocytes with the microtubule destabilizing agent trifluralin (1 μM, 24 h) (16). This treatment caused disassembly of the tubulin bundles, as indicated by the diffuse labeling with Tubulin Tracker (Fig. S1, *Right*). The morphology of the gametocytes was perturbed, but they remained somewhat elongated. Interestingly, this treatment did not restore the ability of the infected RBCs to pass through the microbead mesh (Fig. 1). This result indicates that factors other than (or in addition to) the microtubule cytoskeleton are responsible for the rigidification of stage III gametocytes.

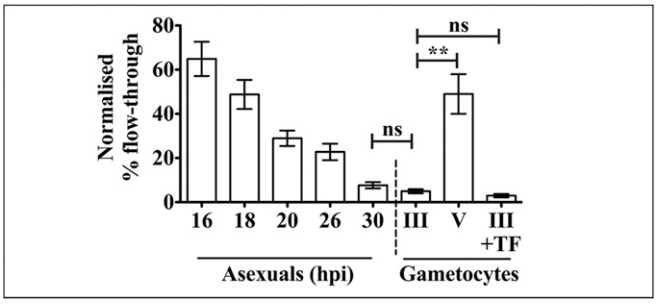

Fig. 1. Filterability of asexual and sexual *P. falciparum* and effect of microtubule destabilization. Asexual stage-infected RBCs at different hours after invasion, stage III (day 6) gametocytes (with or without 24-h trifluralin treatment) and stage V (day 10) gametocytes (~10% parasitemia) were passaged though microbeads. The filterability was determined by comparing the parasitemia in the flow-through and applied samples. Data represents the mean ± SE from three separate experiments, each in triplicate. Unpaired *t* tests were used to determine significance. $^{**}P \leq 0.01$; ns, not significant ($P > 0.05$).

AFM Reveals an Altered Organization of the RBC Membrane Skeleton in Gametocytes. To assess changes to the nanostructure of the RBC membrane, we imaged the skeletal meshwork at the cytoplasmic surface (10, 17). Uninfected RBCs or RBCs infected with trophozoites or stage III or V gametocytes were adhered to glass coverslips. Nonadherent parts of the cells were sheared away, and remnant host RBC membranes were imaged by using AFM (Fig. 2*A*). The meshwork was skeletonized, and the lengths of individual spectrin cross-members and mesh sizes were assessed manually (*SI Materials and Methods* and Fig. S2). In uninfected RBCs, the average spectrin length is 51 ± 9 nm (Fig. 2*B*), in agreement with previous reports (10, 18). In trophozoites and stage III gametocytes, a significant increase in spectrin length was observed (61 ± 14 and 62 ± 8 nm, respectively; $P < 0.0001$) (Fig. 2*B*). By contrast in stage V gametocytes, the membrane skeleton was significantly contracted (average spectrin length, 42 ± 12 nm; $P < 0.0001$). Similarly, the average mesh size increased in RBCs infected with trophozoites ($P < 0.05$) and stage III gametocytes ($P < 0.01$), but decreased from stage III to V gametocytes.

Actin Is Relocated to Maurer's Clefts, with Differential Docking onto the RBC Membrane in Trophozoites and Gametocytes. Previous studies of trophozoites have reported relocation of RBC actin molecules from the skeleton into filaments extending to Maurer's clefts (12); however, actin remodeling and Maurer's cleft tethering has not been examined in gametocytes. In stage III gametocytes prepared for immuno-electron tomography, we observed structures with a characteristic Maurer's cleft morphology (Fig. 3*A*). These organelles are labeled with antibodies recognizing the Maurer's cleft marker, ring exported protein-1 (REX1) (best appreciated in the translations through the electron tomogram (Movie S1) and rotations of the rendered features (Movie S2). In pore-forming toxin-permeabilized samples prepared for immunofluorescence microscopy, anti-REX1 antibodies recognized punctate structures in trophozoites and stage III and V gametocytes, but not in uninfected RBCs (Fig. 3*B*, cyan), confirming the presence of Maurer's clefts. In these permeabilized gametocyte-infected RBCs, the host compartment was flattened and the Maurer's clefts were lined up in a "string of beads" pattern on one side of the parasite. Western analysis of gametocyte samples further confirmed the presence of a band of the expected size for REX1 (Fig. S3*B*).

Two different antiactin antibodies exhibited a weak homogeneous pattern of labeling in uninfected RBCs (Fig. 3*B*, yellow

MICROBIOLOGY

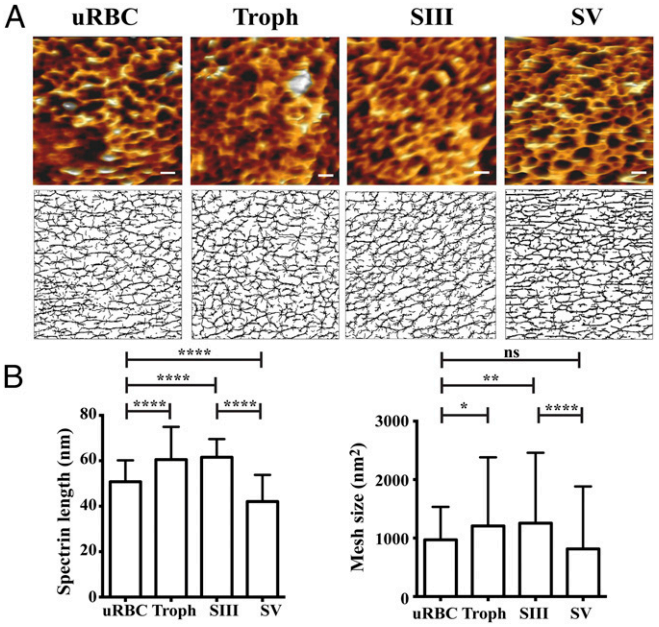

Fig. 2. AFM analysis of the RBC membrane skeleton. (*A*) High-resolution images of the inner surface of an uninfected RBC (uRBC), an infected RBC at trophozoite stage, and stage (S) III and V gametocytes, captured in tapping mode. Corresponding skeletonized images are shown in the lower panels and in Fig. S2 *C* and *D*. (Scale bars: 100 nm.) (*B*) AFM images were analyzed (in a blinded manner) to estimate spectrin length and mesh size (mean ± SD). Differences were assessed by using a one-way ANOVA. ns, not significant ($P > 0.05$); *$P \leq 0.05$; **$P \leq 0.01$; ****$P \leq 0.0001$.

and Fig. S3*C*, yellow), indicating poor access of the antibody to membrane skeleton-located actin. By contrast, when these two antibodies were used to label trophozoite and stage III gametocyte-infected RBCs, a punctate accumulation of the actin signal was observed at the REX1-labeled structures (Fig. 3*B* and Fig. S3*C*; 87% of clefts dual-labeled in stage III gametocytes), consistent with recruitment of actin to the Maurer's clefts. The high level of the fluorescence signal suggests that the Maurer's cleft-located actin exhibits enhanced exposure of the antibody-binding site. No signal was observed when only the secondary antibodies were used (Fig. S3*D*). The level of actin at the Maurer's clefts in stage V gametocytes was much lower (Fig. 3*B* and Fig. S3*C*; 6% of clefts dual-labeled).

To determine whether the Maurer's cleft-associated actin is involved in tethering these organelles to the host RBC membrane, we examined infected RBCs that had been tightly attached to glass coverslips and then subjected to shearing. Actin-labeled Maurer's clefts remained attached to the remnant RBC membranes in trophozoites, but were lost in both stage III and V gametocytes (Fig. 3*C*). Similarly, time-lapse imaging of live BODIPY-TR-ceramide–labeled cells revealed immobile Maurer's clefts in trophozoite-infected RBCs (Movie S3), but mobile clefts in stage III gametocytes (Movie S4). Although the path for diffusion is constrained to the region of the Laveran's bib in stage V gametocytes (Movie S5), the clefts do not appear to be directly connected to the RBC membrane. Together, the data are consistent with reorganization of the actin component of the RBC membrane in both asexual and sexual stage-infected RBCs, but with actin-promoted tethering of Maurer's clefts to the RBC membrane only in asexual-infected RBCs.

Lateral Mobility of Band 3 Is Altered During Asexual and Sexual Blood Stage Development. To further investigate changes in the molecular organization of the RBC membrane, we assessed the lateral mobility of band 3. Band 3 (1.2×10^6 copies per cell) can be specifically labeled with eosin-5′-maleimide at a reactive lysine within the anion channel. We used confocal microscope-based photobleaching protocols (19) to monitor band 3 lateral diffusion. A region of interest on the surface of the RBC was exposed to a focused laser beam, and images were recorded after the bleach pulse (Fig. S4*A*). The fluorescence recovery within the bleached region was significantly lower and slower in trophozoite-infected RBCs (Fig. S4*B*, blue, triangles) than in uninfected RBCs in the same sample (red, diamonds). Stage III gametocytes also exhibited a significantly lower fluorescence recovery than uninfected RBCs (Fig. S4*B*). Interestingly, the lateral mobility of eosin–band 3 was markedly increased in stage V gametocytes, reaching a level similar to that in uninfected RBCs in the same sample (Fig. S4*B*).

It was not possible to directly determine the diffusion coefficient (D) and mobile fraction (f_{mob}) of band 3 from the data obtained, because of continuing recovery of the fluorescence signal at longer time points. Although it is possible that changes in both D and f_{mob} contribute to the altered fluorescence recovery, to obtain information about relative changes in band 3 mobility, we fixed D to 0.0028 $\mu m^2/s$ (19) and floated f_{mob}. The combined uninfected RBC datasets returned an f_{mob} value of 0.40 ± 0.03, in good agreement with published values (19). For the trophozoites and stage III gametocyte datasets, f_{mob} values of 0.20 and 0.18, respectively, were obtained. By contrast, in stage V gametocytes, band 3 exhibited an f_{mob} value (0.33) similar to uninfected RBCs ($P = 0.1$).

Chemical Modulation of the Membrane Skeleton Enhances Filterability and Band 3 Diffusion in Stage III Gametocytes. The F-actin depolymerizing drug cytochalasin D has been shown to destabilize Maurer's cleft-associated actin filaments in trophozoite-infected RBCs (12). Here, we found that treatment of trophozoites with 1 or 10 μM cytochalasin D (2 h) was associated

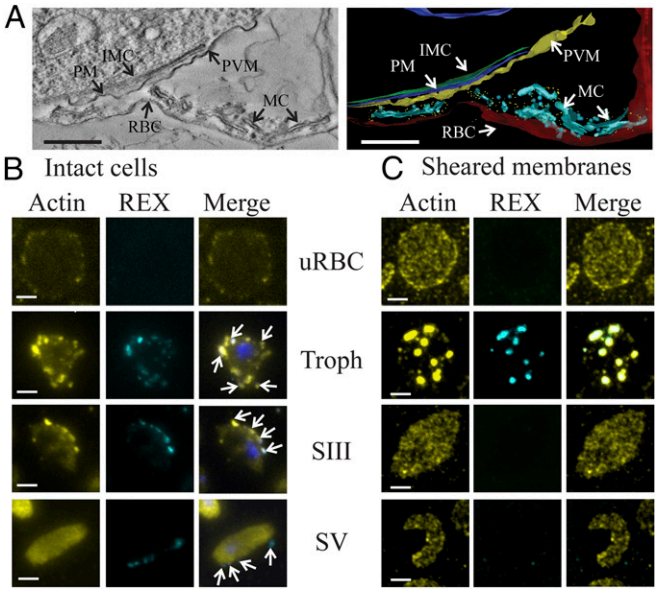

Fig. 3. Maurer's cleft organization and actin remodeling. (*A*) Stage IV Equinatoxin II-permeabilized gametocytes were labeled with anti-REX1 and protein A-gold. A 0.8-nm virtual electron tomogram section shows Maurer's clefts decorated with anti-REX1. A rendered model shows the Maurer's clefts (MC; cyan), RBC membrane (red), the inner membrane complex (IMC; green), the parasite membrane (PM; blue), parasitophorous vacuole membrane (PVM; yellow), and gold particles (gold). (Scale bars: 250 nm.) (*B* and *C*) Immunofluorescence microscopy of Equinatoxin II-permeabilized (*B*) or sheared (*C*) uninfected RBCs, trophozoites, and gametocytes labeled with anti-β-actin (yellow), and REX1 (cyan).

with a small, though not significant, increase in eosin–band-3 fluorescence recovery (Fig. 4*A* and Fig. S5*A*), suggesting that the actin remodeling may be partially reversible during asexual development. Treatment of stage III gametocytes had a more dramatic effect (Fig. 4*A* and Fig. S5*A*). The fluorescence recovery was restored to a value similar to that of uninfected RBCs. This finding suggests that actin reorganization may underlie the altered membrane properties of gametocytes and that this reorganization is largely reversible. By contrast, treatment of stage V gametocytes (or uninfected RBCs) with cytochalasin D did not further increase band 3 mobility (Fig. 4*A* and Fig. S5*A*). It is important to note that these effects do not appear to result from compromised parasite viability, because we have previously shown that short-term cytochalasin treatment does not prevent gametocyte maturation (20).

Similarly, treatment with cytochalasin D significantly (P = 0.002) increased the filterability of stage III gametocytes (Fig. 4*B* and Fig. S5*B*), but did not significantly enhance the already-high filterability of stage V gametocytes and had no effect on trophozoites (Fig. 4*B* and Fig. S5*B*).

A Composite Model Predicts the Physical Consequences of Changes in RBC Membrane Organization. We recently developed a CGMD model to simulate the RBC membrane (8). The CGMD model hybrids a one-agent-thick lipid bilayer model (21) and a spectrin network model (22) by introducing vertical linkages that represent integral proteins (*SI Materials and Methods* and Fig. 5 *A*–*C*). The model is computationally much more efficient than full-atom models, while remaining capable of predicting changes in the mechanical properties of the RBC membrane due to molecular structure remodeling. Here, we extend this model to simulate the shear responses of the infected RBC membrane during gametocytogenesis.

We informed the model with the measured data for spectrin length and meshwork size, taking the uninfected RBC membrane as a reference (Fig. 5 *B*, *i* and *C*, *i*). We used this model to estimate the shear response of the RBC membrane at different stages of parasite development. To compute the shear modulus, a piece of RBC membrane (~600 × 600 nm; Fig. 5*A*) was subjected to simple shear at a rate of $\dot{\gamma} = 2.97 \times 10^5\ s^{-1}$, where γ is the engineering shear strain (see ref. 8 for methods). Fig. 5 *D*, *i* shows the shear stress–strain response of the uninfected RBC membrane, with spectrin end-to-end and contour lengths of 51 and 190 nm, respectively [based on lengths measured in this study and by cryo-EM (18)]. Shearing generates negligible viscous stress in the lipid bilayer, owing to its fluid nature, and the shear resistance is mainly contributed by the spectrin network with a shear modulus of ~9.0 μN/m in the low-strain regime ($0 < \gamma < 0.4$) and ~16.0 μN/m in the high-strain regime ($0.7 < \gamma < 1.0$).

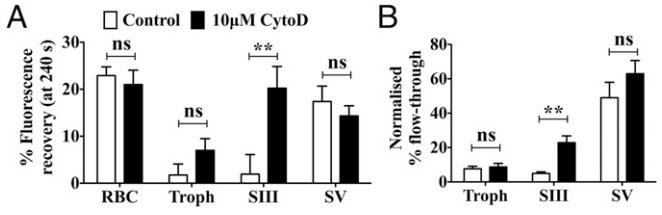

Fig. 4. Effect of cytochalasin D on band-3 lateral mobility and cell filterability. Uninfected and infected RBCs were treated with or without 10 μM cytochalasin D for 2 h. (*A*) Recovery of fluorescence within a bleached region in eosin–maleimide-labeled RBCs was determined 240 s after the bleach pulse (Figs. S4 and S5). (*B*) Samples were passaged though microbeads and filterability was determined by comparing the parasitemia in the flow-through and applied samples. Three individual experiments were performed for *A* and *B*, and data represent the mean ± SE for at least 12 (*A*) or 6 (*B*) samples per treatment group. ns, not significant ($P > 0.05$); $^{**}P \leq 0.01$.

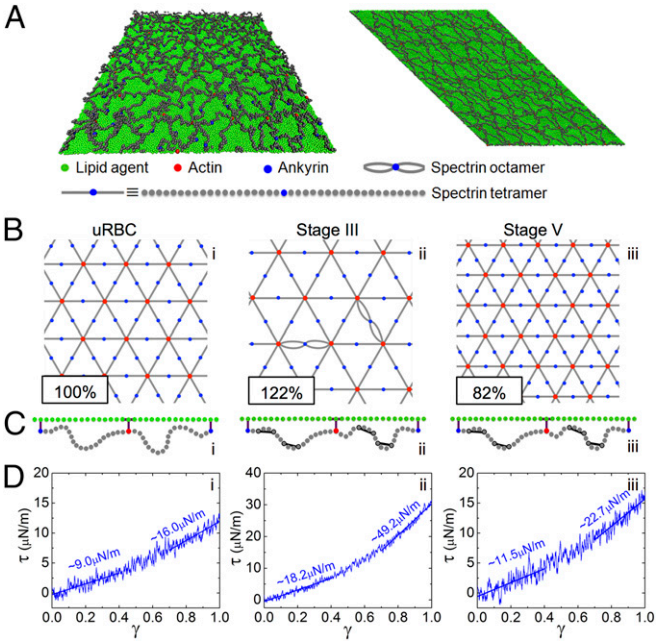

Fig. 5. Modeling of RBC membrane skeleton rearrangements. (*A*) The composite CGMD model of the human RBC membrane comprises a lipid bilayer model and a spectrin network model. Green, lipid agents; blue, ankyrin; red, actin; gray, spectrin beads. (*B*) Lateral organization of the spectrin network model in uninfected RBCs (*i*), stage III gametocytes (*ii*; actin mining, spectrin remodeling, and entropic effects); and stage V gametocytes (*iii*; skeletal shrinkage; entropic effects). (*C*) Vertical associations between the lipid bilayer and the spectrin network. Enhanced constraints between neighboring spectrin beads are indicated by bars. (*D*) Effects of spectrin network remodeling on the shear responses ($\dot{\gamma} = 2.97 \times 10^5\ s^{-1}$) for normal (*i*), stage III gametocyte (*ii*), and stage V gametocyte (*iii*) spectrin meshworks.

The extracted shear moduli fall within the range of experimental data [4–10 μN/m at small shear strain (<0.4); 14–20 μN/m at large shear strain (~1.0) (23)].

We then sought to apply the model to simulate the stage III gametocyte-infected RBC membrane. We assumed the level of actin mining is similar in asexual and midstage sexual parasites. In stage III gametocytes, the increased (on average 22% larger) end-to-end length of spectrin cross-members and meshwork size is modeled as stretched spectrin tetramers converging on 20% fewer actin junction points (8). The final configuration represents global remodeling of the network, with a decrease in the number of junction points and an increase in the distance between neighboring junction points (Fig. 5*B*). To keep the total number of spectrin heterodimers unchanged, 20% of spectrin tetramers were replaced by spectrin octamers (Fig. 5 *B*, *ii*).

We also sought to incorporate into the model a factor describing the enhanced level of interaction between the membrane skeleton and the lipid bilayer. In our previous work, we considered the effects of vertical interactions in the context of trophozoites, where these interactions are expected to be concentrated at the knobs, and we modeled the knobs as rigid regions of the bilayer (~50 nm in radius). We found that the increased vertical interactions lead to a marked increase in stiffness (8). In contrast, gametocytes lack knobs. We found that altering the number of vertical linkages to regions of bilayer with the same properties as in uninfected RBCs does not lead to a significant increase in membrane rigidity (Fig. S6). This finding is due to the fact that, although the lipid bilayer particles surrounding the vertical links have strong short-range connections and form stiff aggregates, the length scale of this effect is only ~4 nm. These stiff, but small-sized, aggregates exert negligible resistance to shear deformation

MICROBIOLOGY

as they are immersed in the fluid lipid bilayer particles and can diffuse freely.

We next considered the possibility that the vertical links modulate the connectivity of the spectrin subunits. Arguably, the deposition of proteins to form the vertical links may locally constrain the configuration of the spectrin tetramer, thus lowering the configurational entropy of the tetramer and subsequently increasing the shear modulus. It is anticipated that such interactions would be distributed across the entire membrane surface. To take into account the loss of spectrin tetramer flexibility, we introduced horizontal linkages within each tetramer, with each linkage covering four neighboring tetramer beads (four constraints per tetramer) (Fig. 5 *C*, *ii*).

For stage III gametocytes, increasing the end-to-end length of spectrin tetramers by 22% and replacing 20% of spectrin tetramers with spectrin octamers led to a 43% increase in shear modulus (from 16.0 to 22.9 μN/m) at the high shear strain regime compared with the uninfected RBC (Fig. S7 *C*, *i*). Introducing four horizontal linkages in each tetramer results in near doubling of the shear modulus (from 16.0 to 31.5 μN/m; Fig. S7 *C*, *ii*). (See Fig. S8 for an analysis of the effects of individual horizontal linkages.) A combination of the three effects—i.e., the change in the end-to-end length of spectrin tetramers, replacing 20% of spectrin tetramers with octamers, and the presence of the horizontal linkages—resulted in a nearly 100% increase in the shear modulus at low-strain regime and a >200% increase in the high-strain regime (Fig. 5 *D*, *ii*). Of note, the shear modulus increase from the combined effects is not a simple superimposition of the individual effects, indicating interamplification of the factors and inherent nonlinearity of the system. The calculated shear modulus at the high-strain regime approached the values (~50–80 μN/m) determined for stage II–III gametocytes (5). This finding suggests that spectrin remodeling and constraints on the spectrin flexibility can account for observed changes in the deformability of the infected RBC membrane in midstage gametocytes.

In stage V gametocytes, the reduced (~18% smaller) end-to-end length of spectrin cross-members and meshwork size is modeled as shortened spectrin tetramers converging on the same number of actin junction points as in the uninfected RBC membrane (Fig. 5 *B*, *iii*). The horizontal linkages are kept (Fig. 5 *C*, *iii*) or removed (Fig. S7 *C*, *iii*) to model the presence or absence of constraints due to binding of exported proteins. Keeping the horizontal linkages in the spectrin tetramers, but introducing the observed 18% decrease in the end-to-end length of the spectrin tetramers, results in a shear modulus only slightly higher than that in uninfected RBCs (Fig. 5 *D*, *iii*). Release of the horizontal linkages further increased the RBC membrane deformability (Fig. S7 *C*, *iii*), with a slightly lower shear modulus than that of the uninfected RBCs. The reduced end-to-end length of the spectrin tetramers appears to be the dominant factor that restores the deformability of the RBC membranes in stage V gametocytes.

Discussion

Developing gametocytes exhibit reduced deformability that coincides with their sequestration in the spleen and bone marrow (5). One might anticipate that the microtubule skeleton that is assembled within the elongating parasite would contribute to the reduced cellular deformability of midstage gametocytes. Surprisingly, an herbicide, trifluralin, that is known to depolymerize *P. falciparum* tubulin, did not increase their ability to passage through a meshwork of beads. This finding suggests that the parasite microtubule skeleton is not the major contributor (or at least not the only contributor) to cellular deformability in stage III gametocytes.

We used AFM to image the membrane skeletons of gametocytes and traced individual spectrin cross-members to obtain a detailed map of the organization of the meshwork. Fully extended spectrin tetramers have a length of ~190 nm (18), but in the context of uninfected RBCs, we estimated a spectrin length of ~50 nm, in agreement with previous reports (10, 11, 18). We used a manual method to measure meshwork size in a manner that accounts for the physical size of the skeletal elements. The measured size (970 nm^2) is consistent with a triangle with ~50-nm sides, but significantly lower than values estimated previously, using thresholding methods (10). The average spectrin contour length and meshwork size were increased by 20–30% in trophozoites and stage III gametocytes, but decreased by 18% in stage V gametocytes, indicating reversible molecular rearrangements.

We found that RBC actin is relocated to Maurer's clefts in both trophozoites and stage III gametocytes; however, the Maurer's clefts are not tethered to the RBC membrane in gametocytes, perhaps due to the absence of knobs, which act as anchoring points in asexual infected RBCs (12). The consequent stretching of the spectrin tetramers to converge on a reduced number of junction points is consistent with the observed reorganized skeleton meshwork.

The lateral diffusion of band 3 is restricted by interactions within the plane of the bilayer and by both direct and indirect interactions with the membrane skeleton. For example, estimates of the level of attachment of band 3 dimers to the spectrin meshwork via ankyrin or adducin range from 50% to 70% (9). The lateral mobility of the band 3 population that is not directly linked to the membrane skeleton is also slowed because weaker interactions between the cytoplasmic domain of band 3 and the skeletal meshwork "corral" its movement. Previous studies have shown that band 3 mobility is compromised in RBCs infected with asexual-stage parasites (19). In this work, we found a similar increase (~40%) in the immobile fraction in stage III gametocytes. By contrast, stage V gametocytes exhibited a similar band 3 mobile fraction to uninfected RBCs.

Given that it is not expressed, KAHRP cannot be responsible for band 3 immobilization in gametocytes. Indeed, band 3 mobility has been shown to be compromised in both knob-plus and -minus trophozoites (19); thus, factors other than KAHRP deposition are clearly involved. We propose that the altered band 3 mobility results directly or indirectly from the reorganization of actin and the consequent reorganization of the spectrin meshwork. For example, junction point reorganization may constrain the flexibility of the spectrin molecules, both stretching them and bringing them closer to the lipid bilayer, resulting in increased corralling of band 3 within microdomains.

To examine the role of actin in remodeling the infected RBC membrane, we treated cells with cytochalasin D. Cytochalasin D is a cell-permeable mycotoxin that binds to the slow-growing ends of actin filaments with high affinity ($K_d \sim 2$ nM) and inhibits both the polymerization and depolymerization at this end (24). Cytochalasin D also binds with low affinity to G-actin ($K_d = 2$–20 μM), which can inhibit the binding of interacting proteins (24) and induce actin dimer formation. This process can result in the nucleation of new actin filaments, but a decrease in the final extent of polymerization. The multiple effects on actin dynamics can lead to different effects on the net level of actin polymerization under different cellular conditions.

We found that treatment of uninfected RBCs with cytochalasin D had no effect on filterability or band 3 mobility. This finding indicates that junction point-associated F-actin is not readily depolymerized, presumably due to stabilization by protein 4.1R, adducin, and tropomyosin (9). Interestingly, cytochalasin D treatment greatly increased the mobility of band 3 in stage III gametocytes, as well as increasing their filterability. Filterability was not increased to the level of stage V gametocytes, indicating that parasite shape and rigidity factors also affect filterability. Filterability was not increased in trophozoites. One possible explanation for this finding is that Maurer's cleft-associated actin filaments are capped by connections into the knobs in trophozoites, but unprotected in gametocytes. Treatment with cytochalasin D may promote the reassembly of the actin into junction complexes within the RBC cytoskeleton of stage III gametocytes. However, it is also

possible that cytochalasin D influences RBC membrane properties in other ways.

In an effort to understand the biomechanical consequences of alterations in the RBC membrane organization, we used a CGMD model to correlate molecular-level structural modifications with membrane shear modulus (elasticity) (8). We previously modeled the skeletal rearrangements in trophozoites as an expanded network with stretched spectrin tetramers and octamers converging on a reduced number of actin junction points. In trophozoites, the enhanced vertical linkages to regions of stiffened membrane (i.e., knobs) are predicted to contribute substantively to the membrane rigidity (8). However, gametocytes lack knobs, and we found that increased linkage into a fluid bilayer is not predicted to directly affect membrane rigidity. Instead, we postulated that the increased linkages are accompanied (or caused) by deposition of parasite-derived proteins onto the membrane skeleton, which might constrain the flexibility of the spectrin tetramers. We found that incorporation of entropic effects into the model yielded predicted values of shear modulus that are comparable with literature values.

In trophozoites, we anticipate that knob-independent membrane rigidity effects operate in parallel with the knob-dependent effects, which could explain why knob-minus parasites are still markedly more rigid than uninfected RBCs (13). Importantly, the entropic effect, caused by binding of proteins to spectrin, may be reversible, underpinning the rigidity reversal that accompanies the transition of gametocytes from stage III to V.

It is interesting to consider what is causing the reorganization of the membrane skeleton. The switch in cellular deformability during the transition from stage III to V gametocytes has been shown to be accompanied by the dissociation of a family of proteins known as the SubTelomeric Variable ORF (STEVOR) proteins from the infected RBC membrane (4) and by enhanced cAMP-dependent kinase-mediated protein phosphorylation (25). The molecular basis of these effects remains to be elucidated, but could involve direct or indirect effects on spectrin elasticity and/or actin organization. Proteins such as skeleton-binding protein-1 and PfEMP1 trafficking protein 1 have been proposed as potential spectrin-interacting proteins in trophozoites. The roles of these proteins in gametocytes have not been studied, but both are expressed. Further dissection of the roles of exported parasite-encoded proteins will be required to fully understand the molecular basis of the membrane skeleton reorganization.

In summary, we have observed remodeling of both lateral and vertical interactions within the gametocyte host RBC membrane skeleton and provided a model of how these changes could lead to altered biomechanical properties. The ability of *P. falciparum* to manipulate the properties of the mature human RBCs in a sophisticated manner may underpin its enhanced virulence compared with other *Plasmodium* species. For example, *Plasmodium vivax* is restricted to reticulocytes, which exhibit a less densely packed membrane skeleton and a lower shear resistance (26). The reversible reprograming of the host cell skeleton has possible parallels in other systems such as *Trichomonas*, pathogenic bacteria, and viruses (27–29). An increased understanding of host cell remodeling processes may point to new ways of tackling these important human pathogens.

Materials and Methods

Methods for parasite culture and gametocyte preparation, fluorescence, electron microscopy, AFM, fluorescence recovery after photobleaching, cell deformability studies, and CGMD modeling are provided in *SI Materials and Methods*.

ACKNOWLEDGMENTS. L.T. and M.W.A.D. thank Dr. Eric Hanssen (Advanced Microscopy Facility), Dr. Paul McMillan (Biological Optical Microscopy Facility), and Emma McHugh (University of Melbourne) for help with imaging. R.C. thanks Prof. Chwee Teck Lim and the Singapore-MIT Alliance for Research and Technology Center (funded by the National Research Foundation, Singapore) for granting access to AFM facilities and laboratory infrastructure. L.T. and M.W.A.D. were supported by the Australian Research Council and National Health and Medical Research Council. T.C., M.A., and R.C. were supported by Singapore University of Technology and Design Grants SRLS13049 and SUTD-ZJU/RES/02/2013. Y.Z., C.J.H., and S.L.Z. were supported by National Science Foundation Grants CMMI-0754463 and CBET-1067523.

1. World Health Organization (2015) *World Malaria Report, 2015* (WHO, Geneva).
2. Dixon MW, Dearnley MK, Hanssen E, Gilberger T, Tilley L (2012) Shape-shifting gametocytes: How and why does *P. falciparum* go banana-shaped? *Trends Parasitol* 28(11):471–478.
3. Sinden RE (1982) Gametocytogenesis of *Plasmodium falciparum* in vitro: An electron microscopic study. *Parasitology* 84(1):1–11.
4. Tibúrcio M, et al. (2012) A switch in infected erythrocyte deformability at the maturation and blood circulation of *Plasmodium falciparum* transmission stages. *Blood* 119(24):e172–e180.
5. Aingaran M, et al. (2012) Host cell deformability is linked to transmission in the human malaria parasite *Plasmodium falciparum*. *Cell Microbiol* 14(7):983–993.
6. Dearnley MK, et al. (2012) Origin, composition, organization and function of the inner membrane complex of *Plasmodium falciparum* gametocytes. *J Cell Sci* 125(Pt 8): 2053–2063.
7. Mohandas N, Gallagher PG (2008) Red cell membrane: Past, present, and future. *Blood* 112(10):3939–3948.
8. Zhang Y, et al. (2015) Multiple stiffening effects of nanoscale knobs on human red blood cells infected with *Plasmodium falciparum* malaria parasite. *Proc Natl Acad Sci USA* 112(19):6068–6073.
9. Mankelow TJ, Satchwell TJ, Burton NM (2012) Refined views of multi-protein complexes in the erythrocyte membrane. *Blood Cells Mol Dis* 49(1):1–10.
10. Shi H, et al. (2013) Life cycle-dependent cytoskeletal modifications in *Plasmodium falciparum* infected erythrocytes. *PLoS One* 8(4):e61170.
11. Millholland MG, et al. (2011) The malaria parasite progressively dismantles the host erythrocyte cytoskeleton for efficient egress. *Mol Cell Proteomics* 10(12):M111.010678.
12. Cyrklaff M, et al. (2011) Hemoglobins S and C interfere with actin remodeling in *Plasmodium falciparum*-infected erythrocytes. *Science* 334(6060):1283–1286.
13. Glenister FK, Coppel RL, Cowman AF, Mohandas N, Cooke BM (2002) Contribution of parasite proteins to altered mechanical properties of malaria-infected red blood cells. *Blood* 99(3):1060–1063.
14. Tibúrcio M, et al. (2013) Early gametocytes of the malaria parasite *Plasmodium falciparum* specifically remodel the adhesive properties of infected erythrocyte surface. *Cell Microbiol* 15(4):647–659.
15. Deplaine G, et al. (2011) The sensing of poorly deformable red blood cells by the human spleen can be mimicked in vitro. *Blood* 117(8):e88–e95.
16. Kaidoh T, Nath J, Fujioka H, Okoye V, Aikawa M (1995) Effect and localization of trifluralin in *Plasmodium falciparum* gametocytes: An electron microscopic study. *J Eukaryot Microbiol* 42(1):61–64.
17. Sinha A, Chu TT, Dao M, Chandramohanadas R (2015) Single-cell evaluation of red blood cell bio-mechanical and nano-structural alterations upon chemically induced oxidative stress. *Sci Rep* 5:9768.
18. Nans A, Mohandas N, Stokes DL (2011) Native ultrastructure of the red cell cytoskeleton by cryo-electron tomography. *Biophys J* 101(10):2341–2350.
19. Parker PD, Tilley L, Klonis N (2004) *Plasmodium falciparum* induces reorganization of host membrane proteins during intraerythrocytic growth. *Blood* 103(6):2404–2406.
20. Hliscs M, et al. (2015) Organization and function of an actin cytoskeleton in *Plasmodium falciparum* gametocytes. *Cell Microbiol* 17(2):207–225.
21. Yuan H, Huang C, Li J, Lykotrafitis G, Zhang S (2010) One-particle-thick, solvent-free, coarse-grained model for biological and biomimetic fluid membranes. *Phys Rev E Stat Nonlin Soft Matter Phys* 82(1 Pt 1):011905.
22. Li J, Lykotrafitis G, Dao M, Suresh S (2007) Cytoskeletal dynamics of human erythrocyte. *Proc Natl Acad Sci USA* 104(12):4937–4942.
23. Park Y, et al. (2008) Refractive index maps and membrane dynamics of human red blood cells parasitized by *Plasmodium falciparum*. *Proc Natl Acad Sci USA* 105(37): 13730–13735.
24. Shoji K, Ohashi K, Sampei K, Oikawa M, Mizuno K (2012) Cytochalasin D acts as an inhibitor of the actin-cofilin interaction. *Biochem Biophys Res Commun* 424(1):52–57.
25. Ramdani G, et al. (2015) cAMP-signalling regulates gametocyte-infected rrythrocyte deformability required for malaria parasite transmission. *PLoS Pathog* 11(5):e1004815.
26. Liu J, Guo X, Mohandas N, Chasis JA, An X (2010) Membrane remodeling during reticulocyte maturation. *Blood* 115(10):2021–2027.
27. Delorme-Axford E, Coyne CB (2011) The actin cytoskeleton as a barrier to virus infection of polarized epithelial cells. *Viruses* 3(12):2462–2477.
28. Fiori PL, Rappelli P, Addis MF, Mannu F, Cappuccinelli P (1997) Contact-dependent disruption of the host cell membrane skeleton induced by *Trichomonas vaginalis*. *Infect Immun* 65(12):5142–5148.
29. Ruetz TJ, Lin AE, Guttman JA (2012) *Shigella flexneri* utilize the spectrin cytoskeleton during invasion and comet tail generation. *BMC Microbiol* 12:36.